

A method to estimate actual infrastructure-induced mortality by integrating sampling biases

Guillermo Gomez-Peña^{1*†}, Marcello D'Amico^{1†}, Carlos Rodríguez¹, Jacinto Román¹,
Alberto García-Rodríguez¹, Eloy Revilla¹, María Paniw¹

¹ Estación Biológica de Doñana CSIC – Calle Américo Vespucio 26, 41092 Seville, Spain

* Corresponding author

guillermo.gomez@ebd.csic.es

[†] Shared first authorship

Running headline

Bayesian latent-state models for roadkill estimates

Acknowledgments, data availability, conflict of interest and author contribution statements

This study has been funded by the Spanish Ministry for the Ecological Transition and the Demographic Challenge MITECO, through the SAFE Project – Stop Atropellos de Fauna en España to the Estación Biológica de Doñana EBD-CSIC. GGP has been supported by the JAE Intro 2022 (JAEINT_22_02345) and JAE Pre 2023 (SOLAUT_00055805) scholarship programs from the Spanish National Research Council CSIC. MD has been supported by Juan de la Cierva - Incorporación (IJC2019-039662-I) from the Spanish Ministry of Science, Innovation and Universities MICIU, and the project “Plan Complementario de I+D+i en el área de Biodiversidad (PCBIO)”, funded by the European Union within the framework of the Recovery, Transformation and Resilience Plan - NextGenerationEU and by the

26 Regional Government of Andalusia. CR was supported by the SAFE Project. AGR
27 was supported by the Spanish Ministry of Science and Innovation (MICINN) through
28 the SUMHAL Project (LIFEWATCH2019-09-CSIC-13. MP was supported by was
29 supported by the Spanish Ministry of Economy and Competitiveness (MINECO) and
30 by the European Social Fund through the Ramón y Cajal Program (RYC2021-
31 033192-I). Miguel Clavero contributed to the conceptualization of this study. Juan
32 Carlos Rivilla and dozens of volunteers contributed to the field samplings. Land
33 Rover España kindly lent a vehicle. Computer resources were provided by the
34 Deputy General Secretariat for Informatics SGAI-CSIC (Drago HPC) and the
35 Estación Biológica de Doñana EBD-CSIC.

36

37 Supplementary material and the scripts used for making the simulation study and
38 case study have been deposited in a ZIP file and in Figshare (Supplementary
39 material S12 link: <https://figshare.com/s/7c6f92b973683e154b91>, Appendix A link:
40 <https://figshare.com/s/e6e4d1e80b4dae5dc434>, Appendix B link:
41 <https://figshare.com/s/760610fb6997e596f8c7>, and Appendix C link:
42 <https://figshare.com/s/2b8aa6942ae0ff7125df>). These links are also included in the
43 ZIP file in a text document named
44 "Supplementary_material_S16_AppendixA_AppendixB_AppendixC_links.txt". If the
45 manuscript is accepted, all data will be archived in Figshare and all scripts will be
46 uploaded to Zenodo.

47

48

49

50

51 **Abstract**

52 1. Human infrastructures are among the most impactful wildlife threats. Although
53 estimates of animal mortality by these structures exist over a given period, they
54 typically do not account for several detection biases (i.e., difference between
55 recorded and true mortality). Consequently, true mortality rates may be severely
56 underestimated, as well as their impact on populations and species.

57 2. We present a hierarchical Bayesian latent-state modelling framework that
58 sequentially accounts for three main processes that produce biases in estimating
59 mortality abundance: the probability that a hit animal dies on the surveyed area
60 (carcass location probability), the probability that the carcass remains on the
61 surveyed area until the survey is conducted (carcass persistence probability), and
62 the probability that the carcass is observed during the survey process (carcass
63 observation probability). We employ a comprehensive simulation study where we
64 test the effects of variability in species characteristics, sampling design, latent-
65 state parameters, and prior information on the ability of our model to estimate
66 mortality abundance on roads as total number of roadkills. We then apply our
67 framework on a case study to estimate the total number of roadkills per km in
68 Mediterranean ecosystems while evaluating the cross-efficiency of different
69 sampling methods.

70 3. Our framework accurately recovers the total number of roadkills from
71 simulated census data for most simulation scenarios. We detected the highest
72 disagreement between modelling outcomes and simulated data when variability
73 in simulated carcass persistence probability was high and Bayesian priors were
74 highly diffuse. In the case study, our results show notably high roadkill numbers

75 (e.g., estimating 48.92 per km passerines based on 8.04 observed counts), along
76 with substantial variation across different vertebrate groups. Furthermore, our
77 case study confirms that walking and cycling surveys outperform driving surveys
78 in carcass observation rate and provide complementary information between
79 them, observing partially distinct sets of species and carcass sizes.

80 4. Our modelling framework offers an efficient approach to estimate mortality
81 rates for a wide range of taxa. Optimizing application requires extensive fieldwork
82 for bias estimation and integration. We provide a checklist to help managers to
83 assess when infrastructure-related mortality can be assessed most robustly to
84 prioritize conservation efforts.

85 We have made all data and code available in a ZIP file and on Figshare (links also in
86 ZIP)

87 **1. Introduction**

88 Linear infrastructures such as roads, power lines and wind turbines have become
89 extremely widespread and are expected to increase substantially in the next
90 decades, particularly in developing countries that host rich biodiversity (D'Amico,
91 Catry, et al., 2018; Meijer et al., 2018; Tabassum-Abbasi et al., 2014). This is
92 worrying because linear infrastructures contribute to the decline and even extinction
93 of wildlife populations, and ultimately to biodiversity loss (Barrientos et al., 2021;
94 D'Amico et al., 2019; Pearce-Higgins et al., 2012). In the last decades, this
95 ecological impact has been extensively studied, with the majority of research
96 focusing on infrastructure-induced mortality (Barrientos et al., 2021; D'Amico,
97 Ascensão, et al., 2018; Nazir et al., 2020). Most research has primarily aimed at
98 investigating the spatiotemporal patterns of such mortality (D'Amico et al., 2015; Guil

99 et al., 2015), although a growing body of studies has more recently sought to
100 quantify the magnitude of this threat.

101

102 However, when estimating infrastructure-induced mortality, standard carcass counts
103 may not accurately reflect the total number of individuals affected. This is because
104 the recorded carcasses are the result of a series of sequential processes, including
105 the affected animal remaining near the infrastructure after the mortality event, the
106 carcass persisting until the survey, and finally the observer detecting it (Barrientos et
107 al., 2018; Bech et al., 2012; Román et al., 2024). Not accounting for these three
108 hierarchical processes may lead to multiple nested sources of bias, i.e., mismatch
109 among recorded roadkills and true road mortality due to lack of detection, when
110 inferring infrastructure-induced mortality from carcass surveys (Barrientos et al.,
111 2018; Román et al., 2024). The first of these biases is carcass location bias and
112 concerns missing animals injured by collisions with power lines, wind turbines, or
113 vehicles on roads that die outside the survey area (Bernardino et al., 2018; Román
114 et al., 2024; Smallwood, 2007). The second bias affecting standard mortality surveys
115 along infrastructures is carcass persistence bias, which occurs when carcasses
116 disappear from the survey area over time before a given survey (Barrientos et al.,
117 2018; Borner et al., 2017; Ravache et al., 2024). This is typically due to natural
118 decomposition and environmental factors influencing it (such as weather conditions;
119 Barrientos et al., 2018; Borner et al., 2017), as well as to scavenger activity (DeVault
120 et al., 2017; Dhiab et al., 2023). On roads, carcass persistence can also be impacted
121 by repeated crushing by vehicles and road maintenance (Abra et al., 2018;
122 Barrientos et al., 2018; Santos et al., 2011). Finally, the third bias is carcass
123 observation bias, which occurs when carcasses within the survey area are not

124 detected by observers, typically due to the sampling method used and the observers'
125 level of experience (Barrientos et al., 2018; Borner et al., 2017; Domínguez del Valle
126 et al., 2020). On roads, this bias tends to be particularly pronounced when roadkill
127 surveys are conducted from vehicles compared to those conducted cycling or
128 walking (Delgado et al., 2019; Guinard et al., 2012; Teixeira et al., 2013).

129

130 Although the hierarchical nature of biases in carcass surveys along infrastructures
131 may appear evident, this aspect has received relatively little attention in the scientific
132 literature. While carcass location bias has been largely neglected in mortality
133 estimates (Barrientos et al., 2018; Román et al., 2024), several authors have
134 highlighted the significant underestimation of carcass records due to both
135 persistence and observation bias (Barrientos et al., 2018; Kitano et al., 2023;
136 Teixeira et al., 2013). Nonetheless, not even the hierarchical nature of these two
137 biases has been sufficiently disclosed in the scientific literature. Some notable
138 exceptions relate to road-mortality research, where recent studies have implemented
139 hierarchical statistical models to account for carcass persistence and observation
140 bias combined as latent states when estimating roadkill numbers (Santos et al.,
141 2018), or even extrapolating such estimates to assess the population abundance of
142 the affected species (Fernández-López et al., 2022). However, despite these recent
143 advances, methods that integrate the varying magnitudes of all three biases in
144 carcass surveys are still lacking, hindering the estimation of the total number of killed
145 animals.

146

147 In this study, we developed a Bayesian latent-state modelling framework that can
148 effectively integrate location, persistence, and observation biases into a reliable

149 estimate of actual infrastructure-induced mortality across different vertebrate groups.
150 More specifically, we focused on road mortality and roadkill surveys, as the scientific
151 literature on this topic is more extensive than that available for other infrastructures.
152 Our framework is an extension of Bayesian N-mixture models, which estimate
153 abundances from repeated counts (Royle, 2004). We conducted a simulation study
154 to assess the framework's accuracy in recovering the simulated total number of
155 roadkills for different vertebrate groups and survey methods (walking, cycling, and
156 driving). In this study, we implemented multiple scenarios in which we varied the
157 number of road transects surveyed, the daily variability in roadkill numbers and
158 carcass persistence rate, and finally the certainty of prior expert knowledge on
159 location and persistence bias probabilities, which we integrated into our model. We
160 then applied our model to a case study with real data collected by road surveys in
161 southern Spain.

162 **2. Material and methods**

163 **2.1 General overview**

164 We first describe our Bayesian hierarchical latent-state modelling framework, which
165 quantifies the total number of roadkills by sequentially assessing how carcass
166 location, persistence and observation biases cause deviations in roadkill census data
167 from actual roadkill (i.e., similar to detection biases in abundance estimation from
168 count data (e.g. Barrientos et al., 2018; Smallwood, 2007) (Fig. 1)). We then
169 evaluate the model's performance through a simulation study, testing different
170 roadkill scenarios across different vertebrate groups and conducting a prior
171 sensitivity analysis. Finally, we apply our model to data from a field case study to
172 estimate the total number of roadkills based on empirical census datasets.

173 2.2 Modelling framework

174 We introduce a hierarchical latent-state model to estimate the total number of
175 roadkills, explicitly accounting for the three nested levels of bias: carcass location,
176 persistence, and observation. The model structure is based on the widely used N-
177 mixture models, which estimate abundances from count data while accounting for
178 imperfect detection (Hostetter et al., 2019; Kery & Royle, 2021; Royle, 2004).

179 We model the total number of roadkills $N_{i,t,D}$ across $i = 1 \dots I$ road transects, within $t =$
180 $1 \dots T$ survey periods (with months used as periods in our model, as more frequent
181 surveys are rarely performed), considering a retrospective carcass accumulation
182 period of D days (representing the maximum number of days a carcass remains on
183 the survey area before disappearing). We define $N_{i,t,D}$ as a random Poisson variable
184 sampled from $\lambda_{t,D}$ = mean number of roadkills for the period t over D days:

185 $N_{i,t,D} \sim \text{Poisson}(\lambda_{t,D})$ eqn. 1

186 As $\lambda_{t,d}$, and consequently $N_{i,t,D}$, can vary across months t , our model accounts for
187 seasonal changes in roadkill numbers throughout the year. Note, however, that we
188 do not model variability in $\lambda_{t,d}$ at the transect level i .

189 We assume that $N_{i,t,D} = \sum_{d=1}^D N_{i,t,d}$, where each daily total number of roadkills $N_{i,t,d}$
190 can fluctuate across the days within period D , following the daily $\lambda_{t,d}$ in month t .
191 However, our framework assumes that $N_{i,t,d}$ and $\lambda_{t,d}$ cannot be modelled directly and
192 instead need to be estimated over the maximum persistence time D , as conducting
193 daily road monitoring is too resource-demanding to be feasible.

194 We then define $N2_{i,t,D}$ as the subset of the total number of roadkills ($N_{i,t,D}$) whose
195 carcasses were located on the road survey area after the collision, determined by
196 the probability of a carcass being located on the road (p_L , carcass location
197 probability):

198 $N2_{i,t,D} \sim \text{Binomial}(p_L, N_{i,t,D})$ eqn. 2

199 As for $N_{i,t,D}$, we assume that $N2_{i,t,D} = \sum_{d=1}^D N2_{i,t,d}$. Based on previous studies
200 (Román et al., 2024), we assume that p_L does not vary among days $d = 1 - D$.

201 Subsequently, we define $N3_{i,t,D} = \sum_{d=1}^D N3_{i,t,d}$ as the subset of roadkills located on
202 the road ($N2_{i,t,D}$) that remain on it until the day of the road survey, determined by the
203 cumulative probability of a carcass persisting on the road survey area, weighted by D
204 (p_P , carcass persistence probability)

205 $N3_{i,t,D} \sim \text{Binomial}(p_P, N2_{i,t,D})$ eqn. 3

206 More precisely, if we assume that the carcass persistence probability could be
207 modelled using a survival function d (e.g., a Cox-hazard model as in Santos et al.
208 2011), then $p_P = \int_{d=1}^D S(d)d(d)$, being the average persistence probability from $d = 1$
209 to D (for details, see Supplementary Material S1). For example, if daily $N2_{i,t,d}$ values
210 are known and, for illustration, we set $D = 3$ days (with $d1$, $d2$ and $d3$ denoting days
211 1, 2 and 3 since roadkills occur), our framework can in theory model:
212 $N3_{i,t,d1} \sim \text{Binomial}(p_{Pd1}p_{Pd2}p_{Pd3}, N2_{i,t,d1})$, $N3_{i,t,d2} \sim \text{Binomial}(p_{Pd2}p_{Pd3}, N2_{i,t,d2})$,
213 $N3_{i,t,d3} \sim \text{Binomial}(p_{Pd3}, N2_{i,t,d3})$, where p_{Pd1} , p_{Pd2} and p_{Pd3} are the daily carcass
214 persistence probability on first, second and third days since roadkills occur,
215 respectively.

216 Finally, we define $C_{i,j,t,D,m}$ as the census data, representing the proportion of the total
217 number of roadkills that have persisted in the road survey area during D and are
218 recorded in a given road survey, which depend on the carcass observation
219 probability p_{om} :

220 $C_{i,j,t,D,m} \sim \text{Binomial}(p_{om}, N_{3i,t,D})$ eqn. 4

221 We assume a robust-design road survey (Royle, 2004), and thus $C_{i,j,t,D,m}$ varies by
222 road transect i , by $m = 1 \dots M$ methods used for surveying (here: walking, bike, or
223 vehicle), as well as by month t (the primary sampling occasion), with $j = 1 \dots J$
224 independent sampling replicates each month (secondary sampling occasion). In turn,
225 p_{om} differs depending on the sampling method m used.

226 Equation 4 builds upon the N-mixture model introduced by Royle (2004), where the
227 estimation of p_{om} comes from the variability among the independent sampling
228 replicates for each method from a robust design census dataset. That is, we assume
229 that independent observers sampled a given road transect repeatedly during a given
230 road survey. This allows us to make an independent estimation of the observation
231 probability per method p_{om} .

232 *2.3 Implementation of the model*

233 We implemented our Bayesian hierarchical latent-state modelling framework to run
234 our model, using Markov chain Monte Carlo (MCMC) to estimate the parameters
235 (Hobbs & Hooten, 2015). Carcass location probability p_L and carcass persistence
236 probability p_P parameters are not typically estimated directly in roadkill census data,
237 and therefore we assumed them to be latent parameters. We employed beta-
238 distributed informative priors for p_L and p_P , with different parameter estimates for

239 different vertebrate groups. The beta distribution is ideal for modelling probabilities
240 like p_L and p_P because it is defined on the interval [0,1] and its probability density
241 distribution can take on various shapes, allowing us to represent different levels of
242 prior belief and uncertainty. For each vertebrate group, we defined the α and β
243 parameters of the beta distribution based on a mean estimate for p_L and p_P ,
244 reflecting our prior knowledge, and a standard error (SE) that captured our
245 uncertainty around this knowledge (see sections 2.3.1 and 2.4.2 for more
246 information).

247 Using the respective mean and SE values for p_L and p_P , we calculated the α and β
248 parameters for their prior beta distributions using the method of moments relative to
249 the standard parameterization of the beta distribution. We adopted a non-informative
250 prior for p_{0m} ($p_{0m} \sim \text{Uniform}(0,1)$), and weakly informative priors for $\lambda_{t,D}$ setting the
251 upper limit sufficiently wide to accommodate the expected number of roadkills
252 ($\lambda_{t,D} \sim \text{Uniform}(0,300)$, $\sim \text{Uniform}(0,600)$ or $\sim \text{Uniform}(0,800)$, as detailed in
253 Supplementary Material S2, S3 and S6), this specific upper limit was selected to
254 ensure values remained biologically reasonable, while increasing the computational
255 stability and convergence of the Bayesian models.

256 The MCMC sampling process was conducted in JAGS (Plummer, 2003), operated
257 within the R statistical framework v. 4.2.2 (R Core Team, 2022) through the jagsUI
258 package v. 1.6.2 (Kellner, 2015). To determine model convergence, we used the
259 Gelman–Rubin \bar{R} diagnostic criterion, considering models to have converged when \bar{R}
260 was less than 1.1, following the guidelines by Brooks and Gelman (1998). We also
261 evaluated the effective sample size (ESS) and visually inspected the traceplots of
262 the posterior distributions among the different MCMC chains to check convergence

263 or mixing issues (see Appendix C). For each model run, we used three chains of
264 400,000 iterations with a burn-in period of 100,000 iterations, an adaptive period of
265 100,000 iterations, and a thinning rate of 1,000.

266 2.3.1 *Prior information on carcass location (p_L) and carcass persistence (p_P)*
267 *probability*

268 We assumed that in most roadkill estimation studies carcass location and
269 persistence probabilities estimations were not available and could not be easily
270 estimated from the census data ($C_{i,j,t,D,m}$). They would have to be entirely modelled
271 as latent states based on prior information. Therefore, in both our simulation and
272 case studies, we integrated such priors based on literature data for these two
273 probabilities. Furthermore, given this structural reliance on prior information, we conducted
274 a specific prior sensitivity analysis to evaluate the robustness of our estimates under
275 different prior specifications (see Section 2.4.3).

276 2.3.1.1 *Carcass location probability (p_L)*

277 We obtained information on p_L from a recent publication, in which authors
278 determined the probability of a carcass being located on the road after the collision
279 from direct and indirect first-hand observations of vehicle-animal collisions (Román
280 et al., 2024). Based on their data, we reorganized their 150 observations into 10
281 vertebrate groups (G) using their supplementary material (Amphibians, Reptiles G1,
282 Reptiles G2, Birds/Bats G1, Birds G2, Mammals G1, Mammals G2, Mammals G3,
283 Mammals G4 and Mammals G5; see Table 1). These groups were delineated based
284 on species traits (body size and mobility); consequently, these groups determined
285 the characteristics of observed roadkill numbers and seasonal trends (differences in
286 abundances across months), as well as the maximum days their carcasses remain

287 on the road without disappearing (D), and the average p_L , p_P , and p_{Om} values, as
288 shown in Table 1.

289 We used the observations in Román et al. (2024) to designate a carcass that was
290 located inside the road as success (1) and outside the road as failure (0), and then
291 calculated the mean of successes over each vertebrate group in order to estimate
292 their p_L . In groups where the value of p_L was 1, we assumed the absence of carcass
293 location bias and hence an extremely low probability of being displaced by the
294 collision or being capable of moving after the impact. For this reason, we excluded
295 equation 2 when modelling such groups (i.e., Amphibians, Reptiles G1, Mammals
296 G1, Mammals G2 and Mammals G3 in Table 1), in such cases $N3_{i,t,D}$ being directly
297 dependent on $N_{i,t,D}$ (Supplementary Material S3).

298 **2.3.1.2 Carcass persistence probability (p_P)**

299 Santos, Carvalho, and Mira (2011) was, to our knowledge, the only study providing
300 estimates of mean daily carcass persistence probability (p_{Pd}) for a diverse array of
301 vertebrate groups from Mediterranean habitats, which we were able to adapt to our
302 classification. We used these values to derive p_P (as discussed in section 2.2 and
303 Supplementary Material S1, see also Supplementary Material S2, S3, S6, S8 and S9
304 for R code). Santos, Carvalho, and Mira (2011) did not provide information for
305 "Mammals G5". Nonetheless, based on available scientific literature, we contended
306 that this group likely does not demonstrate carcass persistence bias within a monthly
307 time period between successive roadkill surveys (Barrientos et al. 2018). For this
308 reason, we excluded equation 3 when modelling this group, in these cases $C_{i,j,t,D,m}$
309 being directly dependent on $N2_{i,t,D} = \sum_{d=1}^D N2_{i,t,d}$ (Supplementary Material S4)

310

311 *2.4 Simulation study*

312 We used a simulation study to stress-test under which scenarios our modelling
313 framework accurately estimated the total number of roadkills $N_{t,D}$ and recovered p_L ,
314 p_P and p_{Om} as latent states. The simulation study generated census data $C_{i,j,t,D,m}$
315 based on different biological and observation processes described below.

316 *2.4.1 Principles of census data generation*

317 To generate different census datasets, we followed the nested levels of data as
318 described in the modelling framework section 2.2 ($N \rightarrow N2 \rightarrow N3 \rightarrow C$). The
319 progression through these levels was carried out considering the values of p_L , p_P
320 and p_{Om} specific to each vertebrate group (Table 1), in order to create a range of
321 biologically realistic data.

322

323 We first sampled $N_{i,t,d}$ for each road transect (i), month (t), and day ($d = 1-D$, where
324 D was the maximum carcass persistence period for a given vertebrate group) as a
325 random Poisson variable based on their mean total number of roadkills $\lambda_{t,d}$ (using
326 equation 1). We used expert knowledge to assign variation in month t dimension
327 based on data collected in 2021 and 2022 in southern Spain, which
328 incorporated known seasonal trends for each vertebrate group (Supplementary
329 Material S5).

330 As an example, considering $D = 3$ days, $\lambda_{t,d1}$, $\lambda_{t,d2}$, and $\lambda_{t,d3}$ would be generated
331 (i.e., the mean number of roadkills occurring three days, two days, or the day before
332 the road survey day, respectively). Roadkills on the survey day itself were not

333 considered as surveys typically occur in the first half of the day. Through the Poisson
334 sampling process, we then obtained the respective $N_{i,t,d1}$, $N_{i,t,d2}$ and $N_{i,t,d3}$, being the
335 total number of roadkills three days, two days and one day before the road survey
336 day respectively. From these values, we could obtain the simulated total number of
337 roadkills $N_{i,t,D} = \sum_{d=1}^D N_{i,t,d}$, which we wanted to recover by applying our modelling
338 framework. For Mammals G5 such as ungulates, since we assumed that their
339 carcasses remain on the road survey area all month and their roadkill numbers were
340 low, simulating $N_{i,t,d}$ values along a $D = 30$ days period led to an unrealistically high
341 value for $N_{i,t,D}$. Therefore, here, we simulated a single $N_{i,t,d}$ value for the entire
342 month, such that $N_{i,t,D} = N_{i,t,d}$.

343

344 Next, for vertebrate groups affected by carcass location bias (Table 1), we sampled
345 $N_{2,i,t,d}$ values from their respective $N_{i,t,d}$, from a random binomial distribution with p_L
346 as the probability of success (equation 2).

347

348 Lastly, we sampled $N_{3,i,t,d}$ values from their respective $N_{2,i,t,d}$, from a random
349 binomial distribution with the daily persistence probabilities p_{Pd} as the probability of
350 success (equation 3). For each vertebrate group with their respective p_{Pd} value (see
351 Supplementary material S1), From these $N_{3,i,t,d}$ values we obtained the simulated
352 total number of roadkills that are available to be observed in the survey day $N_{3,i,t,D} =$
353 $\sum_{d=1}^D N_{3,i,t,d}$. For Mammals G5, which were not affected by carcass persistence bias
354 (i.e., $p_P = 1$), $N_{3,i,t,D}$ was directly dependent on $N_{i,t,D}$ (Supplementary Material S4).

355

356 Finally, we sampled census data $C_{i,j,t,D,m}$ from $N_{3,i,t,D}$, from a random binomial
357 distribution with the carcass observation probability, p_{Om} , as the probability of

358 success (equation 4) using $m = 3$ survey methods (i.e. walking, cycling and driving),
359 with $j = 3$ independent sampling replicates per method. We considered the following
360 evidence when assigning p_{0m} values for the different vertebrate groups (in the
361 absence of more concrete data and based on our expert knowledge): (a) we
362 assumed that observation was highest when walking, followed by cycling, and then
363 driving (Guinard et al., 2012; Winton et al., 2018); (b) we assumed that observation
364 for any of the three methods would be low for small vertebrate groups and high for
365 the large, more visible groups (Gerow et al., 2010; Teixeira et al., 2013) (Table 1).

366

367 *2.4.2 Simulation scenarios of variable data*

368 We generated different simulated census dataset for each of the vertebrate groups
369 considered here (Table 1) using scenarios that introduced different levels of
370 parameters variability (Table 2) to assess when our model can recover simulated
371 parameters and when there is a risk of under- or overestimating total roadkills.

372

373 First, we introduced variability in the daily number of roadkills and persistence rates
374 across simulations of $i = 10$ or 100 road transects. Specifically, we introduced
375 variability in the mean daily number of roadkills $\lambda_{t,d}$ by multiplying it by a value
376 sampled from a truncated random Normal distribution (mean = 1; SD = 0, 0.5, or
377 1.5), and similarly applied variability to the daily persistence probability p_{Pd} by
378 sampling from a truncated random Normal distribution (mean = p_{Pd} ; SD = 0, 0.05, or
379 0.15). We didn't add variability to p_L , as we assume p_L doesn't vary among days. We
380 then analysed these datasets using p_L and p_P priors fitted with both a strong
381 informative prior distribution (Standard Error (SE) = 0.05) and a weaker prior
382 distribution (SE = 0.1) to test how uncertainty in the priors affects the recovery of

383 parameters in the presence of variability, as p_L and p_P values are prior-driven. We
384 couldn't simulate $\lambda_{t,d}$ and p_{Pd} variability for Mammals G5 as we simulated a single
385 $N_{i,t,d}$ value for the entire month and this group is not affected by carcass persistence
386 bias, respectively.

387

388 We also simulated vertebrate groups, i.e., "Amphibians" and "Reptiles G1",
389 characterized by a significant peak in roadkill numbers over just a few months, as
390 examples of high seasonal roadkill numbers due to presumed absence or low
391 numbers of roadkills in certain months where animals are not active (monthly
392 abundance from the 2021 and 2022 data collected <5; see Supplementary Material
393 S5). Here, as we assumed that active and inactive periods were independent, we
394 fitted additional models that only included months where monthly abundance from
395 the 2021 and 2022 data collected was > 5 (see Supplementary Material S6). The aim
396 was to see if model performance improved without accounting for the extended
397 periods with very low roadkill counts, compared to the peak abundance months.

398

399 We simulated 20 datasets for each vertebrate group and scenario combination,
400 resulting in 720 simulated datasets per vertebrate group (dataset simulation code is
401 detailed in Supplementary Material S2, S3, S4 and S6).

402

403 *2.4.3 Prior sensitivity*

404 In our Bayesian models, information on p_L and p_P comes entirely from prior
405 knowledge, as the count data alone ($C_{i,j,t,D,m}$) does not contain sufficient information
406 to independently disentangle these intermediate latent processes without external
407 information. Therefore, we conducted a sensitivity analysis to stress-test whether key

408 simulated parameters can be recovered and p_L and p_P are identifiable by using
409 informative vs. uninformative prior knowledge. We again simulated different datasets
410 for each vertebrate group (as described in 2.4.2), but we fixed the following
411 parameters: $i = 10$ road transects, $\lambda_{t,d}$ and p_{0m} values, and $SD = 0$ for both $\lambda_{t,d}$ and
412 p_{Pd} . We then simulated datasets using pairwise combinations of p_L and p_{Pd} as
413 shown in Supplementary Material S7. For each simulated dataset, we then used
414 three prior specifications in Bayesian models: accurate informative priors centered
415 on the p_L and p_P values associated with each simulated data set (Supplementary
416 Material S7); inaccurate informative priors (0.7 if p_L or $p_P < 0.5$ and 0.3 if p_L or $p_P >$
417 0.5); and finally, uninformative priors using a uniform distribution from 0 to 1. Prior
418 precision was set to $SE = 0.05$ (see 2.4.2).

419 We generated 27 scenario combinations per vertebrate group affected by carcass
420 location and persistence bias, leading to 540 simulated datasets per vertebrate
421 group, while 9 scenario combinations were generated for vertebrate groups only
422 affected by carcass location or persistence bias, i.e., 180 simulated datasets
423 (dataset simulation code is detailed in Supplementary Material S8, S9 and S10).

424 All datasets were generated and analysed in R v. 4.2.2 (R Core Team, 2022) .

425 2.4.4 Model evaluation

426 To evaluate the ability of the modelling framework to recover the simulated
427 parameters we compared their Bayesian posterior distribution of parameters $\hat{\theta}_{s,v,sim,t}$
428 with the real known simulated parameter value $\theta_{s,v,sim,t}$. Here, the subscripts
429 denoted $s = 1\dots S$ simulation scenario, $v = 1\dots V$ vertebrate groups, $sim = 1\dots Sim$
430 specific simulation iteration and $t = 1\dots T$ months. We focused on the recovery of $N_{t,D}$

431 $\theta_{s,v,sim,t}$, and p_L , p_P , and p_{om} $\theta_{s,v,sim}$ (note that there was no dimension t as p_L , p_P ,
432 and p_{om} values did not change across t months).

433 We used the Relative Root Mean Squared Error (*RRMSE*) to compare model
434 performance across simulation scenarios and vertebrate groups. *RRMSE*
435 standardizes the error relative to the magnitude of the true parameter, allowing for
436 comparisons between parameters with different scales (e.g., total number of roadkills
437 vs. carcass bias probabilities). It was calculated as shown in the following equation
438 (Rosenbaum et al., 2024):

439
$$\text{RRMSE}(\hat{\theta}_{s,v,sim,t}) = \frac{1}{\theta_{s,v,sim,t}} \sqrt{(E(\hat{\theta}_{s,v,sim,t}) - \theta_{s,v,sim,t})^2 + \text{Var}(\hat{\theta}_{s,v,sim,t})} \quad \text{eqn. 5}$$

440 where $E(\hat{\theta}_{s,v,sim,t})$ was the mean of the Bayesian posterior distribution. Intuitively,
441 *RRMSE* represents the size of the error as a proportion of the true simulated value.
442 An *RRMSE* of 0 indicates perfect accuracy, while a value of 1 implies that the
443 magnitude of the error is equal to the true simulated value itself. Consequently,
444 *RRMSE* values can exceed 1 (or >0 on a logarithmic scale used for graphical clarity)
445 when the estimation error is larger than the parameter being estimated, indicating
446 high uncertainty. In the case of $N_{t,D}$ $\theta_{s,v,sim,t}$ values, we added 1 to all values as
447 $\text{RRMSE}(\hat{\theta}_{s,v,sim,t})$ could not be calculated when $N_{t,D} = 0$ (Supplementary Material
448 S11).

449 In the case of p_L , p_P , and p_{om} , we generalized their *RRMSE* ($\hat{\theta}_{s,v,sim}$) values as the
450 geometric mean of all probability estimates for each vertebrate group
451 ($\overline{\text{RRMSE}}(\hat{\theta}_{s,v,sim})$), as shown in the following equation (Rosenbaum et al. 2024;
452 Supplementary Material S12):

453 $\overline{\text{RRMSE}}(\hat{\theta}_{s,v,sim}) = \prod_{x \in \{p_L, p_P, p_{Om}\}} \text{RRMSE}(\hat{\theta}_{s,v,sim})^{1/|\{p_L, p_P, p_{Om}\}|}$ eqn. 6

454 To ensure that the true known simulated values were recovered, we assessed
455 whether the average true values $N_{t,D} \theta_{s,v,sim,t}$ lay within the 95% credible interval of
456 Bayesian posterior estimates of average $N_{t,D} \hat{\theta}_{s,v,sim,t}$. In contrast for carcass bias
457 probabilities, we assessed whether the true values $p_L, p_P, p_{Om} \theta_{s,v,sim}$ lay within the
458 full range of their pooled respective posterior distributions p_L, p_P , and $p_{Om} \hat{\theta}_{s,v,sim}$.

459 In the prior sensitivity analysis, we also evaluated across the different simulation
460 scenarios whether the true values $\theta_{s,v,sim,t}$ correctly overlapped with the posterior
461 distributions $\hat{\theta}_{s,v,sim,t}$. Specifically, we assessed the accuracy of estimates for the
462 mean number of roadkills for period t over D days $\lambda_{t,D}$ the total number of roadkills
463 $N_{t,D}$, and the carcass observation probabilities per survey method p_{Om} . Additionally,
464 we verified the successful recovery of the p_L and p_P values integrated into the model
465 as priors.

466

467 **2.5 Case study**

468 We applied our modelling framework to estimate the total number of roadkills across
469 $i = 9$ road transects of 3 km each, in three different Mediterranean ecosystems in
470 south-western Spain (Supplementary Material S13).

471 We collected data on these road sections using $M = 3$ different methods carried
472 simultaneously (walking, cycling, and driving), with $J = 2$ independent sampling
473 repetitions per method (thereby guaranteeing a robust sampling design) for each
474 method and $T = 4$ monthly surveys from February to May in 2023. For each 3 km

475 transect, one observer conducted an initial survey, followed by a second observer
476 after a 10-minute break, considering this interval short enough to assume that the
477 roadkill population was closed. Due to administrative and legal requirements, during
478 the initial phase of the driving surveys, the first observer was solely responsible for
479 roadkill sampling while the second focused entirely on driving. In the subsequent
480 transect sampling repetition, the roles were reversed, allowing the driver to also take
481 on the task of searching for roadkill, ensuring both observers made independent
482 samplings. The survey velocity while driving was the minimum allowed on the road.

483 For each roadkill detected, we noted the observer's identity, the surveyed transect,
484 sampling method, observation month and the exact georeferenced location of the
485 roadkill (with less than 10 m error). Roadkills were documented with zenithal
486 photographs and identified to the lowest feasible taxonomic level, although the
487 ultimate goal was to group them into functional groups. However, unlike the
488 Simulation study (Section 2.4.2) where broad theoretical categories were used (e.g.,
489 "Birds and Bats G1"), here we adapted the group nomenclature to strictly reflect the
490 specific taxa actually observed during fieldwork (e.g., "Passerines").

491

492 **3. Results**

493 In our Bayesian model analysis, the \bar{R} statistic consistently showed values below 1.1,
494 indicating good convergence and precise parameter estimations from the MCMC
495 chains (Appendix A; B; C).

496

497 *3.1 Simulation scenarios of variable data*

498 Our outputs demonstrated overall low $RRMSE(\hat{\theta}_{s,v,sim,t})$ values recovering the
499 simulated total number of roadkills $N_{t,D}(\theta_{s,v,sim,t})$ across nearly all scenarios of
500 variability in parameters (Fig. 2; see also Supplementary Material S14 for more
501 detailed plots for each of the vertebrate groups). Nevertheless, the vertebrate groups
502 Reptiles G2, Birds G2, and Mammals G3 showed very high variation in their
503 distributions, ranging from log $RRMSE(\hat{\theta}_{s,v,sim,t})$ values below -1 to over 4 (Fig. 2).
504 Across vertebrate groups, the highest $RRMSE(\hat{\theta}_{s,v,sim,t})$ scores, indicating relatively
505 worse performance of the model in recovering simulated parameters, corresponded
506 to scenarios with high variability in daily persistence probabilities (SD p_{Pd}) (Fig. 2).
507 Additionally, $RRMSE(\hat{\theta}_{s,v,sim,t})$ increased when the SE was high for the prior
508 distributions for p_L and p_P compared with low SE , and increased further when
509 variability in daily mean number of roadkills (SD $\lambda_{t,d}$) was also high (Fig. 2). The
510 number of road transects simulated (10 or 100 transects) had minimal impact on
511 $RRMSE(\hat{\theta}_{s,v,sim,t})$, except for Reptiles G1, where the $RRMSE(\hat{\theta}_{s,v,sim,t})$ decreased
512 notably in the case of full-year datasets, including extended periods of low number of
513 roadkills (Supplementary Material S14). For Amphibians and Reptiles G1,
514 $RRMSE(\hat{\theta}_{s,v,sim,t})$ were lower when limiting the analysis to months when animals are
515 active (abundance peak), compared to when extended periods of low number of
516 roadkills were included in the datasets (Supplementary Material S14).

517

518 Across all scenarios, when the p_L and p_P prior SE was low, the simulated total
519 number of roadkills $N_{t,D}(\theta_{s,v,sim,t})$ was generally well recovered for all vertebrate
520 groups, i.e., was within the 95% credible interval of $N_{t,D}(\hat{\theta}_{s,v,sim,t})$ (Fig. 3a; see
521 Supplementary Material S15 for more detailed plots). However, Reptiles G1 was an

522 exception: when considering full-year datasets with 10 road transects, estimates for
523 this vertebrate group were overestimated in all scenarios, whereas with 100 road
524 transects they were well recovered. Accounting only for the abundance peak led to
525 better fits overall, even though estimates for this vertebrate group were always
526 underestimated. (Supplementary Material S15). On the other hand, when p_L and p_P
527 prior SE was high, the 95% credible interval overlap widened, leading to
528 overestimations across most vertebrate groups (Supplementary Material S15). The
529 only exception were Amphibians and Reptiles G1 accounting only for the abundance
530 peak, where estimates were typically underestimated, resulting in increased
531 uncertainty but reduced underestimation in most scenarios (Supplementary Material
532 S15).

533

534 $\overline{RRMSE}(\hat{\theta}_{s,v,sim})$ scores for p_L , p_P and p_{om} ($\theta_{s,v,sim}$) showed the same relative
535 differences as $RRMSE(\hat{\theta}_{s,v,sim,t})$, being the highest for Reptiles G1, Birds G2 and
536 Mammals G3 under high variability in daily carcass persistence probabilities (SD
537 p_{pd}) (Fig. 4). This was largely due to the fact that the Bayesian hierarchical models
538 could not recover well p_P under high SD p_{pd} and a high p_P prior SE, although p_{om}
539 values were always well recovered, being much more precise in 100 survey sites
540 scenario (Fig. 3b; see Supplementary Material S16 for more detailed plots). The only
541 exception was the Reptiles G1 full-year dataset with 10 road transects, where p_{om}
542 was not recovered although recovery was successful with 100 transects
543 (Supplementary Material S16).

544

545 3.2 *Prior sensitivity analyses*

546 Regarding our Prior Sensitivity Analysis, we observed that when priors are accurate,
547 the posterior distributions correctly overlapped with the true values, accurately
548 estimating the mean number of roadkills for the period t over D days $\lambda_{t,D}$, the total
549 number of roadkills for the period t over D days $N_{t,D}$, and the carcass observation
550 probabilities per survey method p_{0m} , in addition to successfully recovering the p_L and
551 p_P values integrated in the model as priors (Supplementary material S17). In the
552 case of inaccurate and uninformative prior scenarios, the estimation of p_{0m} values
553 remained robust, although the remaining parameters were affected (Supplementary
554 material S17). Specifically, in the case of inaccurate priors, the p_L and p_P values
555 were never recovered (although the model occasionally recovered estimates of $N_{t,D}$
556 and $\lambda_{t,D}$, but with lower accuracy than in accurate prior scenarios (Supplementary
557 material S17). On the other hand, uninformative priors produced extremely wide
558 posterior distributions of p_L and p_P , which resulted in an extreme overestimation of
559 $N_{t,D}$ and $\lambda_{t,D}$. Furthermore, uninformative priors often resulted in model run errors, as
560 impossible values during the Bayesian estimation process were generated
561 (Supplementary material S17).

562

563 3.3 Case study

564 During the sampling period, we recorded a total of 650 different carcasses of 45
565 identified species (386 of these carcasses could only be classified into higher
566 taxonomic groups). For further modelling, we classified these carcasses into the
567 following taxa: 199 lizards, 17 snakes, 217 passerines, 43 small mammals, 72
568 lagomorphs, and 24 carnivores. Although we observed 40 amphibians, 22 medium-
569 sized birds, 12 hedgehogs and 4 big-sized mammals we were unable to estimate the
570 total number of roadkills for these taxa. Standardizing observations across the 27 km

571 surveyed (9 transects \times 3 km), the roadkill rates per kilometre were highest for
572 passerines (8.04/km) and lizards (7.37/km), followed by lagomorphs (2.67/km), small
573 mammals (1.59/km), carnivores (0.89/km), and snakes (0.63/km).

574

575 Our model generated estimates for the total number of roadkills over the 4 months of
576 sampling on our study roads, taking into account prior distributions of p_L and p_P ,
577 alongside the estimated values of p_{Om} for each sampling method used. The
578 estimated roadkill rates per kilometre were 15.22 for lizards (2.07 times higher than
579 observed), 8.84 for snakes (14.03 times higher), 48.92 for passerines (6.08 times
580 higher), 7.64 for small mammals (4.81 times higher), 7 for lagomorphs (2.62 times
581 higher), and 5.49 for carnivores (6.16 times higher) (see Fig. 5). For each vertebrate,
582 p_{Om} estimation is highest for walking survey method p_{Ow} , followed by cycling p_{Oc} ,
583 and is considerably lower for driving p_{Od} . This was particularly evident in lizards,
584 passerines, and lagomorphs, where p_{Ow} was markedly higher compared to the other
585 methods. For lizards and small mammals, the probability of observation was
586 generally low, with values concentrated close to zero when using the driving method
587 (Fig. 6).

588

589 Finally, our data revealed that some carcasses were observed exclusively by one
590 survey method and not by the others: 294 carcasses were only observed using the
591 walking method, 134 by the cycling method, and 1 by the driving method
592 (Supplementary material S18).

593

594 **4. Discussion**

595 *4.1 Integrating biases in surveys of infrastructure-induced mortality*

596 In the present study, we integrated the three intrinsic survey biases of infrastructure-
597 induced mortality (i.e., carcass location, persistence, and observation bias) within the
598 predefined conceptual framework of our modelling approach. Consequently, we were
599 able to infer the actual mortality from carcass census data, which represents a
600 significant step forward in methodological research on this type of impact, with
601 potentially important implications for the conservation of threatened species as well
602 as for taxa providing ecosystem services. Unlike earlier studies that implemented
603 similar statistical approaches, which provided abundance indices (e.g., Fernández-
604 López et al., 2022) or roadkill risk metrics (e.g., Santos et al., 2018), the application
605 of modified Bayesian N-mixture models in our study allowed us to derive actual
606 roadkill estimates while propagating uncertainty throughout the model thanks to the
607 Bayesian approach (Schmelter et al., 2012). Our roadkill estimates were between
608 2.07 and 14.03 times higher than the observed records in the case study (depending
609 on the species group considered), highlighting that road mortality is a far greater
610 threat than previously recognized, especially for species more affected by sampling
611 biases, such as small birds and bats (Barrientos et al., 2018; Román et al., 2024).
612 Since the biases analyzed in this study are very similar to those affecting other
613 infrastructure-induced mortality surveys (Barrientos et al., 2018; Bernardino et al.,
614 2020), it is reasonable to assume that this threat is also underestimated along power
615 lines, wind farms and other linear developments.

616

617 *4.2 Model performance in simulation scenarios*

618 *4.2.1 Impact of variability in daily parameters*

619 Our simulation scenarios of variable data indicate that, under low variability in daily
620 number of roadkills and daily carcass persistence probabilities, the N-mixture model

621 provides reliable estimates of total number of roadkills. However, when we simulated
622 scenarios with high variability in parameters, total number of roadkills were both
623 over- and underestimated, which was reflected in increased Relative Root Mean
624 Square Error (*RRMSE*) values. These reliability results are consistent with findings by
625 Dennis et al. (2015); Duarte et al. (2018); Link et al. (2018) and Monroe et al. (2019),
626 who emphasize that N-mixture models are highly sensitive to excessive variation in
627 model parameters. Consequently, estimates of total number of roadkill should be
628 interpreted with caution in datasets characterized by high variability in parameters
629 (see Table 3). However, despite these inaccuracies in estimating total roadkill
630 numbers, the models consistently yielded reliable estimates of relative numbers
631 across months. This finding supports the “can’t lose” proposition described by Kéry &
632 Royle (2021): even when violations of parametric assumptions compromise the
633 precision of the absolute population size, the N-mixture framework remains a robust
634 tool for inferring relative dynamics. As noted by Barker et al. (2018); Knape &
635 Korner-Nievergelt (2015) and Martijn et al. (2023), such models effectively
636 characterize relative abundance even when data are sparse or variable.

637

638 4.2.2 *Impact of priors information for carcass location and persistence probability*

639 In most current road survey designs, data on carcass location (p_L) and persistence
640 (p_P) probability are not explicitly collected, and these two parameters are not
641 identifiable from count data alone. Thus, the estimation of these specific biases
642 becomes prior-driven; that is, the posterior distributions are dominated by the prior
643 assumptions rather than by the data itself (Banner et al., 2020; Northrup & Gerber,
644 2018). Our simulation scenarios of variable data and prior sensitivity show that weak
645 informative, uninformative or inaccurate prior distributions (i.e., wide distributions

646 with high standard errors, uniform distributions or informative priors intentionally
647 biased away from the true values) propagated uncertainty directly to estimates total
648 number of roadkill or resulted in low recovery and identifiability of simulated carcass
649 location and persistence probability priors by the Bayesian model, an issue
650 highlighted by (Fidino, 2021). This behaviour is consistent with literature on Bayesian
651 mixture models, which warns that inference can become unstable when data are
652 sparse and priors are uninformative (Depaoli, 2013; Depaoli et al., 2017).

653

654 Our results demonstrate that to obtain reliable estimates of the total number of
655 roadkills, future roadkill studies cannot rely on vague priors for carcass bias
656 probabilities; they require informative priors derived from independent empirical data;
657 or, ideally, would incorporate independent data to facilitate the estimation of posterior
658 distributions of these parameters. Thus, research efforts must prioritize collecting
659 auxiliary data to quantify carcass location probability (Román et al., 2024) and
660 persistence rates (Ruiz-Capillas et al., 2015; Santos et al., 2018), as these
661 independent constraints are necessary to anchor the model parameters.

662

663 *4.2.3 Differences among vertebrate groups*

664 When simulated data are highly variable or priors were uninformative, the total
665 number of roadkills can be overestimated, depending on the vertebrate group. The
666 fact that lizards were overestimated when considering full-year datasets with 10 road
667 transects and informative priors is likely due to extremely low persistence and
668 observation probabilities in this group, which resulted in a zero-inflated simulated
669 dataset for analysis. In such cases, a higher sampling efforts (Guillera-Arroita et al.,
670 2010; MacKenzie et al., 2002) and employing a zero-inflated Poisson version of the

671 N-mixture model can yield more accurate results (Joseph et al., 2009; Wenger &
672 Freeman, 2008).

673

674 *4.2.4 Reliability checklist to assess robustness of Bayesian framework in future*
675 *applications*

676 Based on the model's performance across our simulation scenarios, we provide a
677 reliability checklist to guide researchers in ensuring the reliability of total mortality
678 estimates in infrastructure mortality surveys (Table 3). The model generally provides
679 robust estimates of all target parameters when accurate priors are available for the
680 carcass location and carcass persistence probabilities. However, as outlined in the
681 checklist (Table 3), the precision of these estimates may be compromised in
682 scenarios where prior uncertainty or data complexity affect the reliability and
683 performance of the model. In such instances, while carcass observation probability
684 estimates tend to remain robust, the estimates for the total number of roadkills
685 should be approached with caution.

686

687 Future applications must cautiously evaluate and document prior knowledge on
688 carcass location and persistence probabilities and ideally incorporate, auxiliary field
689 experiments to estimate posterior distributions. In addition, we strongly recommend
690 restricting the analysis to the biologically active season for taxa with marked
691 seasonal dynamics (e.g., amphibians, reptiles). Lastly, results must be interpreted
692 with caution when applying these models to datasets where daily roadkill numbers or
693 persistence rates fluctuate drastically. For such highly variable data, estimates
694 should be interpreted as robust indices of relative abundance (Kéry & Royle, 2021).

695

696 Crucially, beyond adhering to this checklist, we strongly recommend that researchers
697 using our Bayesian models to estimate infrastructure mortality perform their own
698 simulations to validate the model's suitability for their specific study system and data.
699 By utilizing the simulation R scripts provided in this study (Supplementary Material
700 S2, S3, S4 and S6), users can easily adapt our specifications to generate simulated
701 datasets that mimic their specific study conditions (e.g., number of survey transects;
702 carcass location, persistence and observation per method probabilities values).

703

704 *4.3 Case study application*

705 Applying the hierarchical modelling framework to empirical data in our case study
706 showed an important increase in the estimated number of roadkills compared to
707 those observed, aligning with the findings of other studies (e.g Teixeira et al. (2013);
708 Winton et al. (2018)). Also, our estimates for carcass observation probabilities align
709 with previous findings in the literature, as it is highest for walking surveys, followed
710 by cycling, and lowest for driving (Guinard et al., 2012; Ogletree & Mead, 2020;
711 Winton et al., 2018), and it is also lower for smaller vertebrate groups and higher for
712 larger, more visible species (Gerow et al., 2010; Teixeira et al., 2013). Our study is
713 the first to compare all three survey methods simultaneously within the same study.
714 We not only demonstrate that walking surveys—while the most effective method—
715 are not perfect and should not be assumed to observe all roadkill events, as was
716 done in Teixeira et al. (2013), but we also show that a significant number of
717 carcasses were missed by walking surveys but observed by cycling. This suggests
718 that walking, cycling, and driving surveys should not be seen as a ranking from best
719 to worst but rather as complementary methods, each with its own advantages and
720 limitations. For example, while walking likely helps observe carcasses directly

721 underfoot, the elevated perspective provided by cycling allows for a broader field of
722 view, making it easier to observe carcasses on the roadside.

723

724 These results highlight that using the driving method in surveys not only reduces the
725 proportion of carcasses observed on the road but can also lead to an overestimation
726 of the total number of collisions. In N-mixture models, lower observation probabilities
727 result in larger extrapolations in the estimated values. Since observation probabilities
728 while driving are extremely low, the estimated total number of roadkills ultimately
729 would be much higher than the real one (Dennis et al., 2015; Hostetter et al., 2019).

730

731 Regarding our case study survey methodology, one important consideration is that,
732 typically, roadkill studies alternate the direction of search and the side of the road
733 randomly in order to cover the area as thoroughly as possible along the
734 infrastructure (D'Amico et al., 2015). However, in our case, as our study was an
735 initial phase of a citizen science project with volunteers, we had to employ a simple
736 and easy sampling method, conducting surveys on only one side of the road and
737 always in the same direction. Although we recognize that this may decrease the
738 carcass observation probability, it would be interesting to investigate in the future
739 whether randomizing the direction and side of the road would actually reduce
740 carcass observation bias.

741

742 *4.4 Limitations and future perspectives*

743 A limitation of our methodology is that it requires extensive knowledge of carcass
744 location, persistence, and observation biases specific to each infrastructure,
745 vertebrate group, and study environment. The bias values for each of these contexts

746 may vary, which is crucial for making accurate estimates in each case. Another
747 limitation of our estimates of total number of roadkills is that they are limited by the
748 maximum number of days a carcass from a specific vertebrate group remains on the
749 road before disappearing (*D*-day period). This means that to estimate the number of
750 roadkill for periods larger than the *D*-day period (e.g., one month or a specific
751 season), we currently simply extrapolate our estimates for the *D*-day period over a
752 larger time window (e.g., 30 days / *D*-day period). Thus, for vertebrate groups with
753 shorter persistence times (such as amphibians and lizards), the extrapolation gap
754 required to cover the unobserved temporal window is significantly larger than for
755 groups with longer persistence times (such as large birds and carnivores). To
756 address the accuracy of monthly extrapolations, roadkill survey frequency should
757 take into account the persistence period of the target vertebrate group. This
758 approach would be particularly useful in studies focused on endangered or high-
759 interest species, due to most studies do not typically follow this method, as they
760 generally assess overall vertebrate mortality (e.g. D'Amico et al., 2015). For species
761 with short persistence times, such as lizards, surveys should be done every day
762 throughout the study season to avoid extrapolation and rely on actual observed data.

763

764 Finally, our modelling framework could be used for animal conservation issues by
765 combining it with population abundance estimation models near to infrastructure,
766 offering a valuable tool to assess what proportion of the study population may
767 succumb to infrastructure-related mortality, such as roads (Barrientos et al., 2021),
768 power lines (Biasotto & Kindel, 2018; D'Amico et al., 2019) and multiple linear
769 infrastructures (Ascensão et al., 2022). This information would facilitate the
770 identification of species or populations more significantly affected by infrastructure-

771 related mortality (e.g. species with very low population sizes and highly susceptible
772 to roadkill), thereby prioritizing conservation efforts.

773

774 **Bibliography**

775 Abra, F. D., Huijser, M. P., Pereira, C. S., & Ferraz, K. M. P. M. B. (2018). How reliable are
776 your data? Verifying species identification of road-killed mammals recorded by road
777 maintenance personnel in São Paulo State, Brazil. *Biological Conservation*, 225, 42–
778 52. <https://doi.org/10.1016/j.biocon.2018.06.019>

779 Ascensão, F., D'Amico, M., & Barrientos, R. (2022). No Planet for Apes? Assessing Global
780 Priority Areas and Species Affected by Linear Infrastructures. *International Journal of
781 Primatology*, 43(1), 57–73. <https://doi.org/10.1007/s10764-021-00207-5>

782 Banner, K. M., Irvine, K. M., & Rodhouse, T. J. (2020). The use of Bayesian priors in
783 Ecology: The good, the bad and the not great. *Methods in Ecology and Evolution*,
784 11(8), 882–889. <https://doi.org/10.1111/2041-210X.13407>

785 Barker, R. J., Schofield, M. R., Link, W. A., & Sauer, J. R. (2018). On the reliability of N-
786 mixture models for count data. *Biometrics*, 74(1), 369–377.
787 <https://doi.org/10.1111/biom.12734>

788 Barrientos, R., Ascensão, F., D'Amico, M., Grilo, C., & Pereira, H. M. (2021). The lost road:
789 Do transportation networks imperil wildlife population persistence? *Perspectives in
790 Ecology and Conservation*, 19(4), 411–416.
791 <https://doi.org/10.1016/j.pecon.2021.07.004>

792 Barrientos, R., Martins, R. C., Ascensão, F., D'Amico, M., Moreira, F., & Borda-de-Água, L.
793 (2018). A review of searcher efficiency and carcass persistence in infrastructure-
794 driven mortality assessment studies. *Biological Conservation*, 222, 146–153.
795 <https://doi.org/10.1016/j.biocon.2018.04.014>

796 Bech, N., Beltran, S., Boissier, J., Allienne, J.-F., Resseguier, J., & Novoa, C. (2012). Bird
797 mortality related to collisions with ski-lift cables: Do we estimate just the tip of the
798 iceberg? *Animal Biodiversity and Conservation*, 35(1), 95–98.

799 Bernardino, J., Bevanger, K., Barrientos, R., Dwyer, J. F., Marques, A. T., Martins, R. C.,
800 Shaw, J. M., Silva, J. P., & Moreira, F. (2018). Bird collisions with power lines: State
801 of the art and priority areas for research. *Biological Conservation*, 222, 1–13.
802 <https://doi.org/10.1016/j.biocon.2018.02.029>

803 Bernardino, J., Bispo, R., Martins, R. C., Santos, S., & Moreira, F. (2020). Response of
804 vertebrate scavengers to power line and road rights-of-way and its implications for
805 bird fatality estimates. *Scientific Reports*, 10(1), 15014.
806 <https://doi.org/10.1038/s41598-020-72059-7>

807 Biasotto, L. D., & Kindel, A. (2018). Power lines and impacts on biodiversity: A systematic
808 review. *Environmental Impact Assessment Review*, 71, 110–119.
809 <https://doi.org/10.1016/j.eiar.2018.04.010>

810 Borner, L., Duriez, O., Besnard, A., Robert, A., Carrere, V., & Jiguet, F. (2017). Bird collision
811 with power lines: Estimating carcass persistence and detection associated with
812 ground search surveys. *Ecosphere*, 8(11), e01966. <https://doi.org/10.1002/ecs2.1966>

813 Brooks, S. P., & Gelman, A. (1998). General Methods for Monitoring Convergence of
814 Iterative Simulations. *Journal of Computational and Graphical Statistics*, 7(4), 434–
815 455. <https://doi.org/10.1080/10618600.1998.10474787>

816 D'Amico, M., Ascensão, F., Fabrizio, M., Barrientos, R., & Gortázar, C. (2018). Twenty years
817 of road ecology: A topical collection looking forward for new perspectives. *European
818 Journal of Wildlife Research*, 64, 1–2.

819 D'Amico, M., Catry, I., Martins, R. C., Ascensão, F., Barrientos, R., & Moreira, F. (2018). Bird
820 on the wire: Landscape planning considering costs and benefits for bird populations
821 coexisting with power lines. *Ambio*, 47(6), 650–656. <https://doi.org/10.1007/s13280-018-1025-z>

823 D'Amico, M., Martins, R. C., Álvarez-Martínez, J. M., Porto, M., Barrientos, R., & Moreira, F.
824 (2019). Bird collisions with power lines: Prioritizing species and areas by estimating
825 potential population-level impacts. *Diversity and Distributions*, 25(6), 975–982.
826 <https://doi.org/10.1111/ddi.12903>

827 D'Amico, M., Román, J., De los Reyes, L., & Revilla, E. (2015). Vertebrate road-kill patterns
828 in Mediterranean habitats: Who, when and where. *Biological Conservation*, 191,
829 234–242.

830 Delgado, J. D., Durán Humia, J., Rodríguez Pereiras, A., Rosal, A., del Valle Palenzuela, M.,
831 Morelli, F., Arroyo Hernández, N. L., & Rodríguez Sánchez, J. (2019). The spatial
832 distribution of animal casualties within a road corridor: Implications for roadkill
833 monitoring in the southern Iberian rangelands. *Transportation Research Part D:
834 Transport and Environment*, 67, 119–130. <https://doi.org/10.1016/j.trd.2018.11.017>

835 Dennis, E. B., Morgan, B. J. T., & Ridout, M. S. (2015). Computational Aspects of N-Mixture
836 Models. *Biometrics*, 71(1), 237–246. <https://doi.org/10.1111/biom.12246>

837 Depaoli, S. (2013). Mixture class recovery in GMM under varying degrees of class
838 separation: Frequentist versus Bayesian estimation. *Psychological Methods*, 18(2),
839 186–219. <https://doi.org/10.1037/a0031609>

840 Depaoli, S., Yang, Y., & Felt, J. (2017). Using Bayesian Statistics to Model Uncertainty in
841 Mixture Models: A Sensitivity Analysis of Priors. *Structural Equation Modeling: A
842 Multidisciplinary Journal*, 24(2), 198–215.
843 <https://doi.org/10.1080/10705511.2016.1250640>

844 DeVault, T. L., Seamans, T. W., Linnell, K. E., Sparks, D. W., & Beasley, J. C. (2017).
845 Scavenger removal of bird carcasses at simulated wind turbines: Does carcass type
846 matter? *Ecosphere*, 8(11), e01994. <https://doi.org/10.1002/ecs2.1994>

847 Dhiab, O., D'Amico, M., & Selmi, S. (2023). Experimental evidence of increased carcass
848 removal along roads by facultative scavengers. *Environmental Monitoring and
849 Assessment*, 195(1), 216.

850 Domínguez del Valle, J., Cervantes Peralta, F., & Jaquero Arjona, M. I. (2020). Factors
851 affecting carcass detection at wind farms using dogs and human searchers. *Journal*
852 *of Applied Ecology*, 57(10), 1926–1935. <https://doi.org/10.1111/1365-2664.13714>

853 Duarte, A., Adams, M. J., & Peterson, J. T. (2018). Fitting N-mixture models to count data
854 with unmodeled heterogeneity: Bias, diagnostics, and alternative approaches.
855 *Ecological Modelling*, 374, 51–59. <https://doi.org/10.1016/j.ecolmodel.2018.02.007>

856 Fernández-López, J., Blanco-Aguiar, J. A., Vicente, J., & Acevedo, P. (2022). Can we model
857 distribution of population abundance from wildlife–vehicles collision data? *Ecography*,
858 2022(5), e06113. <https://doi.org/10.1111/ecog.06113>

859 Fidino, M. (2021, August 25). *A gentle introduction to an integrated occupancy model that*
860 *combines presence-only and detection/non-detection data, and how to fit it in*
861 *`JAGS`*. https://masonfidino.com/bayesian_integrated_model/

862 Gerow, K., Kline, N. C., Swann, D. E., & Pokorny, M. (2010). Estimating annual vertebrate
863 mortality on roads at Saguaro National Park, Arizona. *Human-Wildlife Interactions*,
864 4(2), 283–292.

865 Guil, F., Àngels Colomer, M., Moreno-Opo, R., & Margalida, A. (2015). Space–time trends in
866 Spanish bird electrocution rates from alternative information sources. *Global Ecology*
867 and *Conservation*, 3, 379–388. <https://doi.org/10.1016/j.gecco.2015.01.005>

868 Guillera-Arroita, G., Ridout, M. S., & Morgan, B. J. T. (2010). Design of occupancy studies
869 with imperfect detection. *Methods in Ecology and Evolution*, 1(2), 131–139.
870 <https://doi.org/10.1111/j.2041-210X.2010.00017.x>

871 Guinard, É., Julliard, R., & Barbraud, C. (2012). Motorways and bird traffic casualties:
872 Carcasses surveys and scavenging bias. *Biological Conservation*, 147(1), 40–51.
873 <https://doi.org/10.1016/j.biocon.2012.01.019>

874 Hobbs, N. T., & Hooten, M. B. (2015). *Bayesian Models: A Statistical Primer for Ecologists*
875 (STU-Student edition). Princeton University Press.
876 <https://www.jstor.org/stable/j.ctt1dr36kz>

877 Hostetter, N. J., Gardner, B., Sillett, T. S., Pollock, K. H., & Simons, T. R. (2019). An
878 integrated model decomposing the components of detection probability and
879 abundance in unmarked populations. *Ecosphere*, 10(3), e02586.
880 <https://doi.org/10.1002/ecs2.2586>

881 Joseph, L. N., Elkin, C., Martin, T. G., & Possingham, H. P. (2009). Modeling abundance
882 using N-mixture models: The importance of considering ecological mechanisms.
883 *Ecological Applications*, 19(3), 631–642. <https://doi.org/10.1890/07-2107.1>

884 Kellner, K. (2015). jagsUI: a wrapper around rjags to streamline JAGS analyses. *R Package
885 Version*, 1(1).

886 Kery, M., & Royle, J. A. (2021). *Applied Hierarchical Modeling in Ecology: Analysis of
887 Distribution, Abundance and Species Richness in R and BUGS*. Academic Press.

888 Kéry, M., & Royle, J. A. (2021). *Applied Hierarchical Modeling in Ecology: Analysis of
889 Distribution, Abundance and Species Richness in R and BUGS: Volume 2: Dynamic
890 and Advanced Models*. Academic Press.

891 Kitano, M., Smallwood, K. S., & Fukaya, K. (2023). Bird carcass detection from integrated
892 trials at multiple wind farms. *The Journal of Wildlife Management*, 87(1), e22326.
893 <https://doi.org/10.1002/jwmg.22326>

894 Knape, J., & Korner-Nievergelt, F. (2015). Estimates from non-replicated population surveys
895 rely on critical assumptions. *Methods in Ecology and Evolution*, 6(3), 298–306.
896 <https://doi.org/10.1111/2041-210X.12329>

897 Link, W. A., Schofield, M. R., Barker, R. J., & Sauer, J. R. (2018). On the robustness of N-
898 mixture models. *Ecology*, 99(7), 1547–1551. <https://doi.org/10.1002/ecy.2362>

899 MacKenzie, D. I., Nichols, J. D., Lachman, G. B., Droege, S., Andrew Royle, J., & Langtimm,
900 C. A. (2002). Estimating Site Occupancy Rates When Detection Probabilities Are
901 Less Than One. *Ecology*, 83(8), 2248–2255. [https://doi.org/10.1890/0012-9658\(2002\)083%255B2248:ESORWD%255D2.0.CO;2](https://doi.org/10.1890/0012-9658(2002)083%255B2248:ESORWD%255D2.0.CO;2)

903 Martijn, B., Jim, C., Natalie, B., & Thomas, N. (2023). Simulation-based assessment of the
904 performance of hierarchical abundance estimators for camera trap surveys of

905 unmarked species. *Scientific Reports*, 13(1), 16169. <https://doi.org/10.1038/s41598-023-43184-w>

906

907 Meijer, J. R., Huijbregts, M. A. J., Schotten, K. C. G. J., & Schipper, A. M. (2018). Global
908 patterns of current and future road infrastructure. *Environmental Research Letters*,
909 13(6), 064006. <https://doi.org/10.1088/1748-9326/aabd42>

910 Monroe, A. P., Wann, G. T., Aldridge, C. L., & Coates, P. S. (2019). The importance of
911 simulation assumptions when evaluating detectability in population models.
912 *Ecosphere*, 10(7), e02791. <https://doi.org/10.1002/ecs2.2791>

913 Nazir, M. S., Ali, N., Bilal, M., & Iqbal, H. M. N. (2020). Potential environmental impacts of
914 wind energy development: A global perspective. *Current Opinion in Environmental
915 Science & Health*, 13, 85–90. <https://doi.org/10.1016/j.coesh.2020.01.002>

916 Northrup, J. M., & Gerber, B. D. (2018). A comment on priors for Bayesian occupancy
917 models. *PLOS ONE*, 13(2), e0192819. <https://doi.org/10.1371/journal.pone.0192819>

918 Ogletree, K., & Mead, A. (2020). What Roadkills Did We Miss in a Driving Survey? A
919 Comparison of Driving and Walking Surveys in Baldwin County, Georgia. *Georgia
920 Journal of Science*, 78(2). <https://digitalcommons.gaacademy.org/gjs/vol78/iss2/8>

921 Pearce-Higgins, J. W., Stephen, L., Douse, A., & Langston, R. H. W. (2012). Greater
922 impacts of wind farms on bird populations during construction than subsequent
923 operation: Results of a multi-site and multi-species analysis. *Journal of Applied
924 Ecology*, 49(2), 386–394. <https://doi.org/10.1111/j.1365-2664.2012.02110.x>

925 Plummer, M. (2003). JAGS: A program for analysis of Bayesian graphical models using
926 Gibbs sampling. *Working Papers*.

927 R Core Team. (2022). *R: A language and environment for statistical computing*. [R
928 Foundation for Statistical Computing].

929 Ravache, A., Barré, K., Normand, B., Goislot, C., Besnard, A., & Kerbiriou, C. (2024).
930 Monitoring carcass persistence in windfarms: Recommendations for estimating
931 mortality. *Biological Conservation*, 292, 110509.
932 <https://doi.org/10.1016/j.biocon.2024.110509>

933 Román, J., Rodríguez, C., García-Rodríguez, A., Diez-Virto, I., Gutiérrez-Expósito, C.,
934 Jubete, F., Paniw, M., Clavero, M., Revilla, E., & D'Amico, M. (2024). Beyond
935 crippling bias: Carcass-location bias in roadkill studies. *Conservation Science and*
936 *Practice*, 6(4), e13103. <https://doi.org/10.1111/csp2.13103>

937 Rosenbaum, B., Li, J., Hirt, M. R., Ryser, R., & Brose, U. (2024). Towards understanding
938 interactions in a complex world: Design and analysis of multi-species functional
939 response experiments. *Methods in Ecology and Evolution*, 15(9), 1704–1719.
940 <https://doi.org/10.1111/2041-210X.14372>

941 Royle, J. A. (2004). N-Mixture Models for Estimating Population Size from Spatially
942 Replicated Counts. *Biometrics*, 60(1), 108–115. <https://doi.org/10.1111/j.0006->
943 341X.2004.00142.x

944 Ruiz-Capillas, P., Mata, C., & Malo, J. E. (2015). How many rodents die on the road?
945 Biological and methodological implications from a small mammals' roadkill
946 assessment on a Spanish motorway. *Ecological Research*, 30, 417–427.

947 Santos, R. A. L., Mota-Ferreira, M., Aguiar, L. M. S., & Ascensão, F. (2018). Predicting
948 wildlife road-crossing probability from roadkill data using occupancy-detection
949 models. *Science of The Total Environment*, 642, 629–637.
950 <https://doi.org/10.1016/j.scitotenv.2018.06.107>

951 Santos, S. M., Carvalho, F., & Mira, A. (2011). How Long Do the Dead Survive on the Road?
952 Carcass Persistence Probability and Implications for Road-Kill Monitoring Surveys.
953 *PLOS ONE*, 6(9), e25383. <https://doi.org/10.1371/journal.pone.0025383>

954 Schmelter, M. L., Erwin, S. O., & Wilcock, P. R. (2012). Accounting for uncertainty in
955 cumulative sediment transport using Bayesian statistics. *Geomorphology*, 175–176,
956 1–13. <https://doi.org/10.1016/j.geomorph.2012.06.012>

957 Smallwood, K. S. (2007). Estimating Wind Turbine-Caused Bird Mortality. *The Journal of*
958 *Wildlife Management*, 71(8), 2781–2791. <https://doi.org/10.2193/2007-006>

959 Tabassum-Abbasi, Premalatha, M., Abbasi, T., & Abbasi, S. A. (2014). Wind energy:
960 Increasing deployment, rising environmental concerns. *Renewable and Sustainable*
961 *Energy Reviews*, 31, 270–288. <https://doi.org/10.1016/j.rser.2013.11.019>
962 Teixeira, F. Z., Coelho, A. V. P., Esperandio, I. B., & Kindel, A. (2013). Vertebrate road
963 mortality estimates: Effects of sampling methods and carcass removal. *Biological*
964 *Conservation*, 157, 317–323. <https://doi.org/10.1016/j.biocon.2012.09.006>
965 Wenger, S. J., & Freeman, M. C. (2008). Estimating Species Occurrence, Abundance, and
966 Detection Probability Using Zero-Inflated Distributions. *Ecology*, 89(10), 2953–2959.
967 <https://doi.org/10.1890/07-1127.1>
968 Winton, S. A., Taylor, R., Bishop, C. A., & Larsen, K. W. (2018). Estimating actual versus
969 detected road mortality rates for a northern viper. *Global Ecology and Conservation*,
970 16, e00476. <https://doi.org/10.1016/j.gecco.2018.e00476>
971

972 **Figures and tables**

973

974 Table 1. Descriptive characteristics of the different vertebrate groups used to
975 simulate roadkill numbers, including examples of species, their features of observed
976 roadkill numbers and their seasonal variation, maximum days their carcass remains
977 on the road without disappearing (D), probability of their carcass being located on
978 the road (p_L), average probability across D of their carcass persisting on the road
979 (p_P) and carcass observation probability (p_{Om}) by walking (p_{ow}), cycling (p_{oc}) and
980 driving (p_{odr}) survey method.

Vertebrate groups	Example	Observed roadkill abundance	Seasonal variation	D (days)	p_L	p_P	p_{Om}		
							p_{ow}	p_{oc}	p_{odr}
Amphibians	Small	Frequently	High	2	1	0.36	0.5	0.3	0.02

	amphibians such as <i>Bufo spinosus</i> or <i>Epidalea calamita</i>	observed							
Reptiles G1	Small reptiles such as <i>Psammodromus algirus</i> or <i>Timon lepidus</i>	Frequently observed	High	1	1	0.54	0.5	0.3	0.02
Reptiles G2	Medium-sized ophidians such as <i>Malpolon monspessulanus</i> or <i>Zamenis scalaris</i>	Frequently observed	High	3	0.43	0.36	0.7	0.5	0.1
Birds/Bats G1	Small birds such as <i>Carduelis carduelis</i> or bats	Frequently observed	Low	3	0.36	0.36	0.6	0.4	0.05
Birds G2	Medium-sized birds such as <i>Alectoris rufa</i> or large birds as <i>Asio otus</i>	Rarely observed	Low	10	0.69	0.34	0.8	0.6	0.2
Mammals G1	Small mammals such as <i>Mus spretus</i> or <i>Rattus rattus</i>	Frequently observed	Low	3	1	0.36	0.6	0.4	0.05
Mammals G2	Medium-sized mammals such as <i>Oryctolagus cuniculus</i> or <i>Lepus</i>	Frequently observed	Low	4	1	0.35	0.8	0.6	0.2

	<i>granatensis</i>								
Mammals G3	Mammals with keratinous structures such as <i>Erinaceus europaeus</i>	Rarely observed	Low	12	1	0.34	0.8	0.6	0.2
Mammals G4	Medium-sized carnivores as <i>Felis catus</i> or <i>Vulpes vulpes</i>	Frequently observed	Low	14	0.65	0.34	0.9	0.7	0.3
Mammals G5	Big mammals as <i>Sus scrofa</i> or <i>Cervus elaphus</i>	Rarely observed	Low	30	0.5	1	1	0.9	0.8

981

982 Table 2. Simulation scenarios to generate roadkill census data, including levels of
 983 variation and justification for the scenario choice. $\lambda_{t,d}$ = daily mean number of roadkills
 984 in month t for each specific day d across D (maximum persistence), p_{Pd} = daily
 985 carcass persistence probability, SD = Standard Deviation and SE = Standard Error.

Parameter	Levels	Justification
Nº road transect	10/100	N-mixture models can be sensitive to the spatial replication of count surveys (Kery & Royle, 2021). Increasing the number of transects can enhance the precision of estimates by improving the spatial representativeness of the data
SD in $\lambda_{t,d}$	0/0.5/1.5	Since we model the total number of roadkills as the sum over the maximum persistence period (D), we aim to know how this modelling approach impacts our

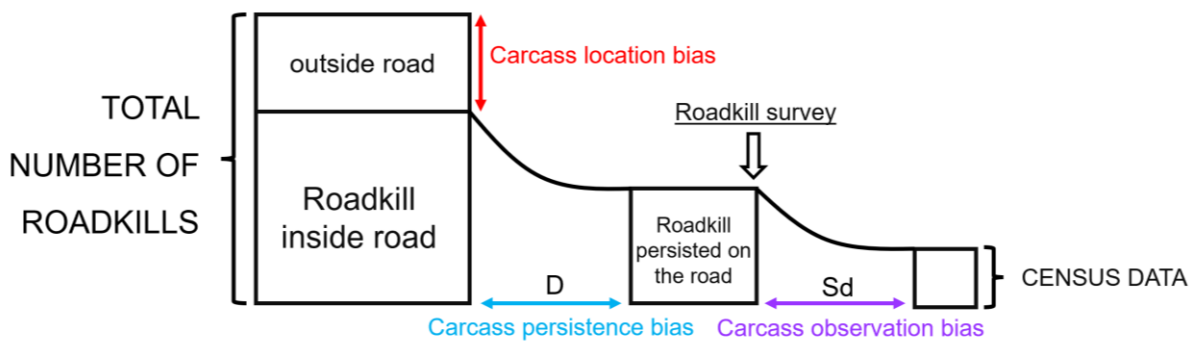
		estimates when daily values show no variation, moderate variation, or high variation
SD in p_{pd}	0/0.05/0.15	Since we model the carcass persistence probability as the average of carcass persistence probabilities over the maximum persistence period (D), we aim to know how this modelling approach impacts our estimates when daily values show no variation, moderate variation, or high variation
SE in priors p_L and p_P	0.05/0.1	Since we model our prior beta-distribution α and β parameters for a p_L and p_P from their mean values and a SE that captures our uncertainty around this knowledge, we aim to know how low and high uncertainty impacts our estimates

986

987 Table 3: Checklist to assess reliability of our model's absolute infrastructure mortality
 988 estimates. The matrix classifies reliability into three levels: Robust (green), Caution
 989 (yellow), and High risk of erroneous outputs (red), based on three critical modelling
 990 constraints: Priors information (specifically for carcass location and persistence
 991 probabilities), variability of parameters in input data, and seasonality of road mortality
 992 events.

Key factors affecting model robustness	Robust	Caution	High risk of erroneous outputs
Prior information (carcass location and persistence probabilities)	<u>Accurate</u> : Based on literature from same ecosystems and vertebrate group or derived from independent field experiments.	<u>Inaccurate</u> : Based on literature but from different ecosystems or vertebrate groups. <u>Result</u> : Non-identifiability. Better use only as relative index.	<u>Weak informative or uninformative</u> : wide distributions with high SE or Uniform distributions (0-1). <u>Result</u> : Non-identifiability, model run errors, and mortality overestimation. Use only as relative index.
Variability of parameters in input data	<u>Low variability</u> : Daily carcass persistence and daily mortality numbers are relatively constant.	<u>Moderate variability</u> : Variability is present but remain within a moderate order of magnitude. <u>Result</u> : Increased uncertainty in estimates.	<u>High variability</u> : Extreme variability in daily carcass persistence or daily mortality numbers. <u>Result</u> : Use only as relative index.
Seasonality of road mortality events	<u>Active season only</u> : Dataset restricted to biologically active months of specific vertebrate groups.	<u>Full year with low seasonality</u> : Vertebrate groups with continuous activity along the year (e.g., some mammals). <u>Result</u> : Increased uncertainty in estimates.	<u>Full year with high seasonality</u> : vertebrate groups with inactive periods (e.g. amphibians/lizards). <u>Result</u> : Increased uncertainty and reduced accuracy in estimates.

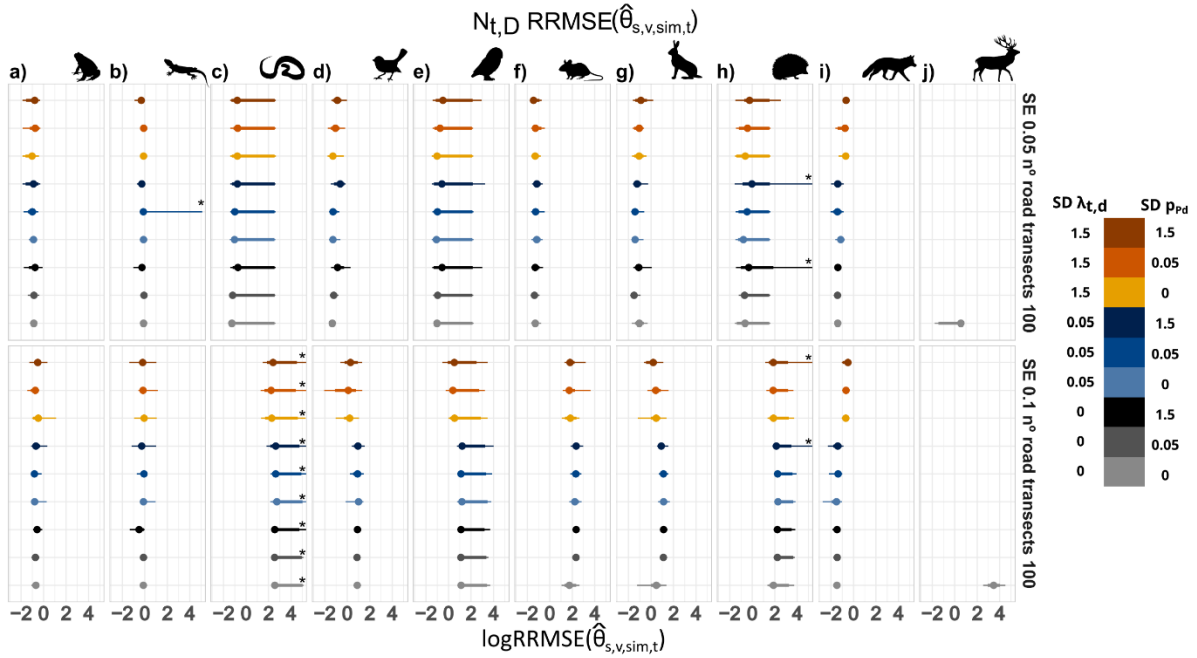
993



994

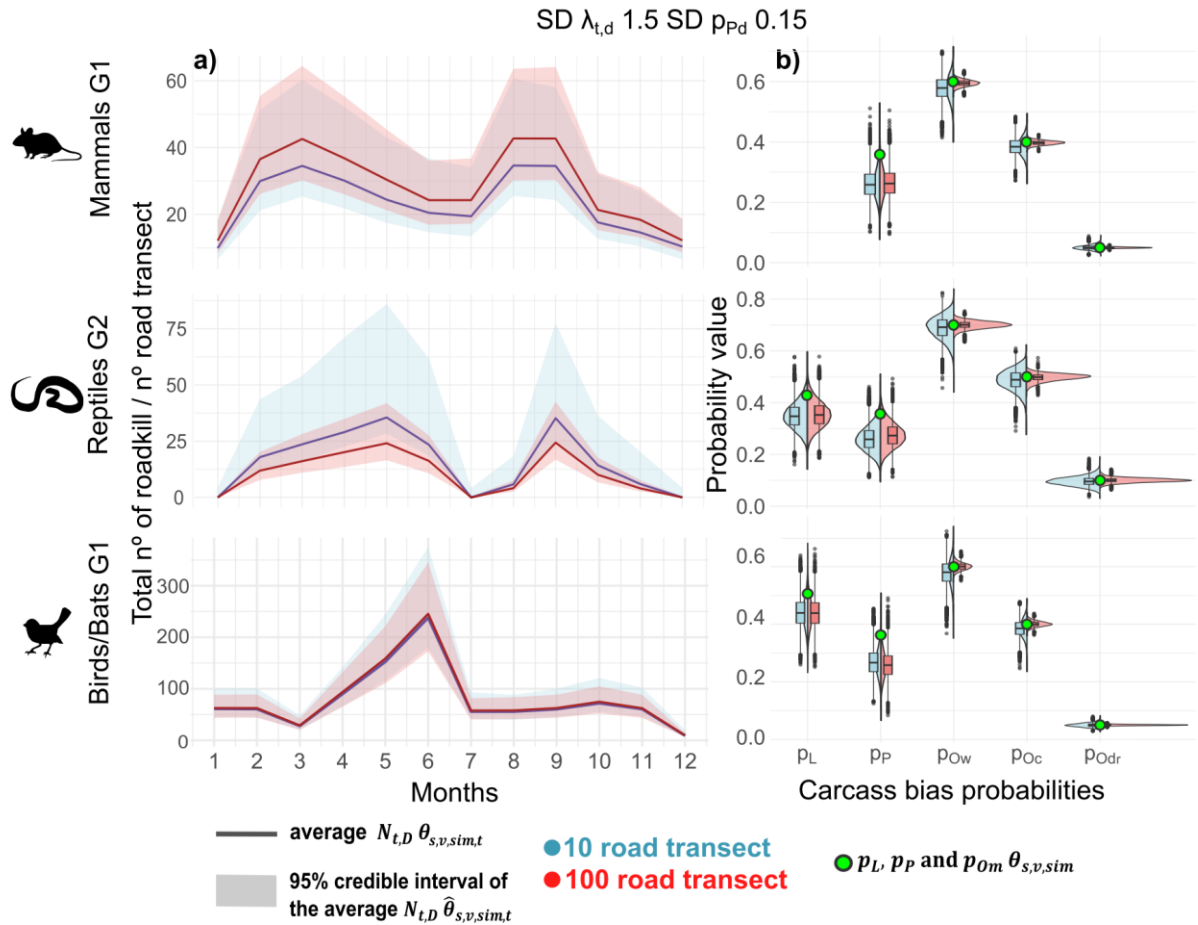
995 Figure 1. Roadkill survey bias framework. This diagram illustrates how three types of
 996 survey bias (carcass location bias, carcass persistence bias, and carcass
 997 observation bias) impact the census data of roadkill within the surveyed road. These
 998 theoretical different sizes of the squares in the diagram symbolize the quantity of
 999 roadkill that would be available at each nested level of the framework. Additionally, D
 1000 represents the time elapsed between the roadkill event and the maximum days a
 1001 carcass remains on the road without disappearing until survey day, where carcass
 1002 persistence bias occurs, while S_d represents the survey duration, during which
 1003 observational bias occurs.

1004



1005

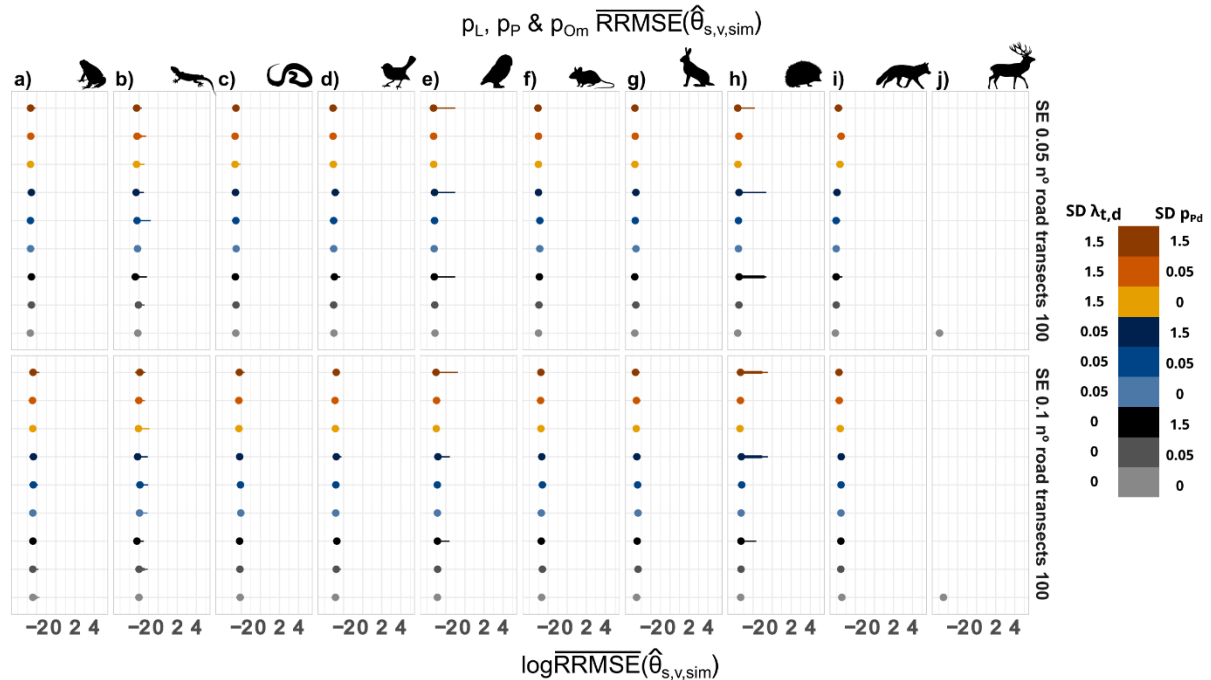
1006 Figure 2: $N_{t,D} RRMSE(\hat{\theta}_{s,v,sim,t})$ values (Equation 5), where log values <0 indicate
 1007 high accuracy of the model, log values $=0$ indicate that the magnitude of the error
 1008 equals the true simulated value, and log values >0 indicates low accuracy of the
 1009 model. This is evaluated across $s = 9$ different scenario combinations of mean daily
 1010 number of roadkills and daily carcass persistence variability ($SD \lambda_{t,d}$ and $SD p_{Pd}$), $v =$
 1011 10 vertebrate groups, $sim = 20$ simulations, $t = 12$ months and $D =$ maximum days a
 1012 carcass remains on the road without disappearing. Each distribution represents
 1013 $N_{t,D} RRMSE(\hat{\theta}_{s,v,sim,t})$ values derived from each sim and t levels described above for
 1014 a) Amphibians, b) Reptiles G1, c) Reptiles G2, d) Birds/Bats G1, e) Birds G2, f)
 1015 Mammals G1, g) Mammals G2, h) Mammals G3, i) Mammals G4 and j) Mammals
 1016 G5. The results are shown for 2 levels of standard error (0.05 or 0.1) for the p_L and
 1017 p_P prior distributions, and for 100 road transects surveyed. Coloured circles
 1018 represent the mean, bold lines for 66% intervals, and thin lines 95% intervals. An
 1019 asterisk (*) in the distributions indicates values exceeding 5 that are part of the
 1020 distribution. Note: Amphibians and Reptiles G1 vertebrate groups models only
 1021 account for peak abundance months, excluding periods of typical absence.



1024 Figure 3: Comparison between the Bayesian estimation distribution of $N_{t,D}$ given
 1025 $\hat{\theta}_{s,v,sim,t}$ and of p_L , p_P and p_{0m} given $\hat{\theta}_{s,v,sim}$, and their true simulated values, $N_{t,D}$
 1026 given $\theta_{s,v,sim,t}$ and p_L , p_P and p_{0m} given $\theta_{s,v,sim}$, for Mammals G1, Reptiles G2, and
 1027 Birds/Bats G1. Here census data were simulated under high variability scenario for
 1028 daily mean number of roadkills ($\lambda_{t,d}$) and daily carcass persistence probability (p_{Pd}),
 1029 considering a SE = 0.05 in p_L and p_P priors. a) Comparison of total number of
 1030 roadkills per transect. Lines represent the average $N_{t,D} \theta_{s,v,sim,t}$ over 20 simulations,
 1031 while the shaded areas show the average 95% credible interval of Bayesian
 1032 posterior estimates $N_{t,D} \hat{\theta}_{s,v,sim,t}$ over the 20 simulated census data. b) Comparison
 1033 of carcass location, persistence and observation probability per method. Green dots
 1034 represent the p_L , p_P and $p_{0m} \theta_{s,v,sim}$ values for m = walking (p_{0w}), cycling (p_{0c}) or

1035 driving (p_{odr}) survey methods. Violin plots combined with boxplots (representing the
 1036 same underlying data) show the pooled p_L , p_P and p_{om} $\hat{\theta}_{s,v,sim}$ over 20 simulated
 1037 census data.

1038

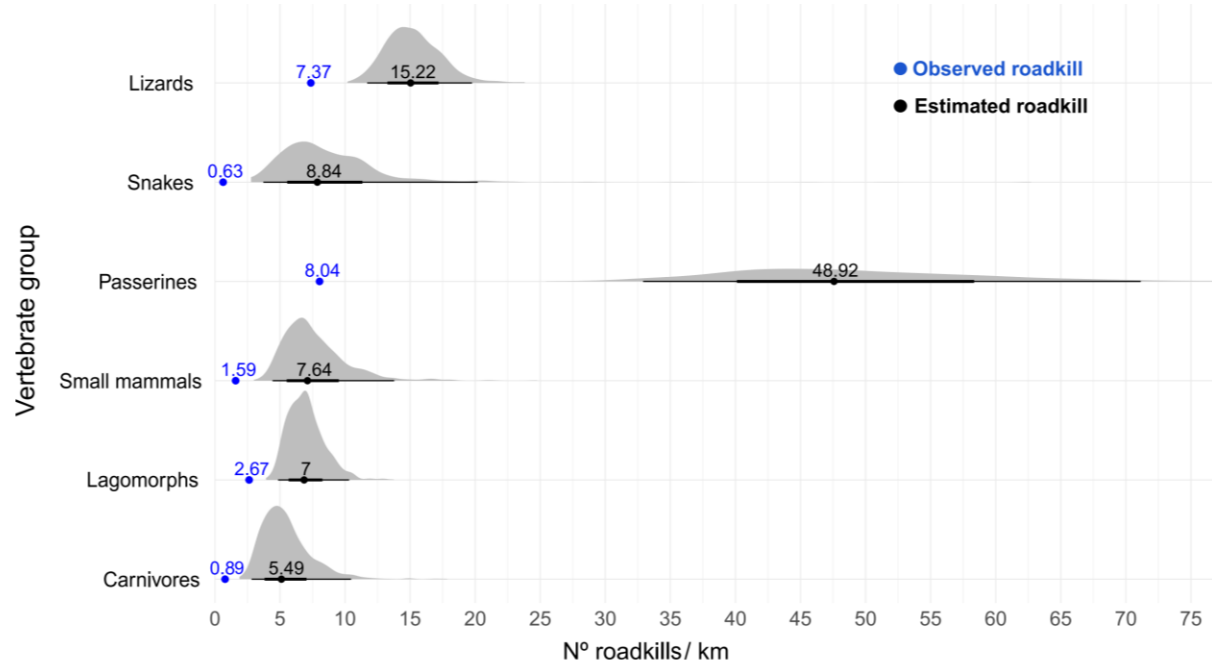


1039

1040 Figure 4: p_L, p_P & $p_{om} \bar{RRMSE}(\hat{\theta}_{s,v,sim})$ (Equation 6), where log values <0 indicate
 1041 high accuracy of the model, log values $=0$ indicate that the magnitude of the error
 1042 equals the true simulated value, and log values >0 indicates low accuracy of the
 1043 model. This is evaluated across $s = 9$ different scenario combinations of daily mean
 1044 number of roadkills and daily carcass persistence variability ($SD \lambda_{t,d}$ and $SD p_{pd}$), $v =$
 1045 10 vertebrate groups, $sim = 20$ simulations and $m =$ walking, cycling and driving
 1046 survey methods. Each distribution represents p_L, p_P & $p_{om} \bar{RRMSE}(\hat{\theta}_{s,v,sim})$ values
 1047 derived from each sim level described above for a) Amphibians, b) Reptiles G1, c)
 1048 Reptiles G2, d) Birds/Bats G1, e) Birds G2, f) Mammals G1, g) Mammals G2, h)
 1049 Mammals G3, i) Mammals G4 and j) Mammals G5. The results are shown for 2
 1050 levels of standard error (0.05 or 0.1) for the p_L and p_P prior distributions, and for 100

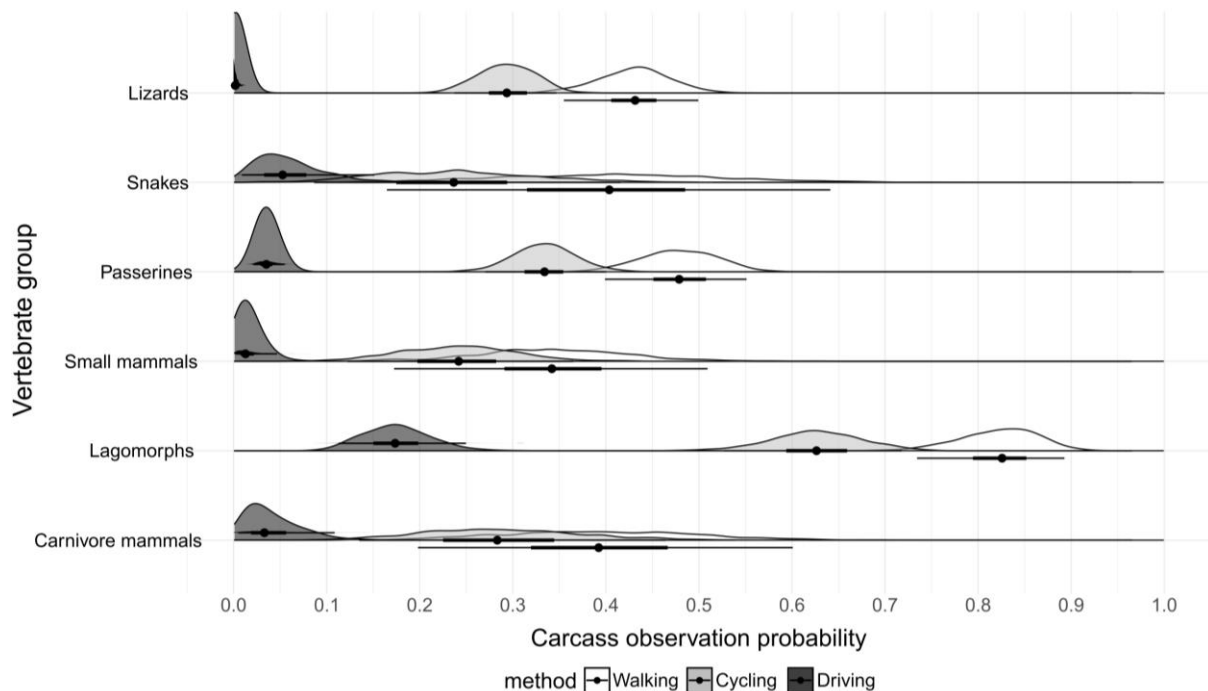
1051 road transects surveyed. Coloured circles represent the mean, bold lines for 66%
1052 intervals, and thin lines 95% intervals. Note: Amphibians and Reptiles G1 vertebrate
1053 groups models only account for peak abundance months, excluding periods of
1054 typical absence.

1055



1056
1057 Figure 5. Observed roadkill rates per kilometer in road surveys (blue) and Bayesian
1058 posterior estimates of total roadkill rates per kilometer (black), derived from
1059 aggregating four monthly census data of the case study, for each vertebrate group.
1060 These estimated roadkill rates are limited to those that occurred within the time
1061 interval where each vertebrate group remains visible on the road without
1062 disappearing. Dots for means, bold lines for 66% credible intervals, and thin lines for
1063 95% credible intervals.

1064



1065

1066 Figure 6. Bayesian posterior distribution of the carcass observation probabilities from
1067 case study, for each considered vertebrate groups. “Walking” means the estimation
1068 of carcass observation probability by walking survey method, “Cycling” by cycling
1069 survey method and “Driving” by driving survey method. Dots for means, bold lines for
1070 66% credible intervals, and thin lines for 95% credible intervals.